Synthesis, Crystal Structure, EXAFS, and Magnetic Properties of *catena*-Poly[μ-tris(4-(2-hydroxyethyl)-1,2,4-triazole-N^1,N^2)copper(II)] Diperchlorate Trihydrate: Relevance with the Structure of the Iron(II) 1,2,4-Triazole Spin Transition Molecular Materials

Yann Garcia,[†] Petra J. van Koningsbruggen,[†] Georges Bravic,[†] Philippe Guionneau,[†] Daniel Chasseau,[†] Giovanni Luca Cascarano,[‡] Jacques Moscovici,[§] Katia Lambert,[§] Alain Michalowicz,[§,||] and Olivier Kahn*[,†]

Laboratoire des Sciences Moléculaires, Institut de Chimie de la Matière Condensée de Bordeaux, UPR CNRS no. 9048, Avenue du Docteur Schweitzer, F-33608 Pessac, France, Istituto di Ricerca per lo Sviluppo di Metodologie Cristallografiche CNR, c/o Dipartimento Geomineralogico, Campus Universitario, 70124 Bari, Italy, Laboratoire de Physique des Milieux Désordonnés, Université Paris XII-Val de Marne, Avenue du Général De Gaulle, 94010 Créteil Cedex, France, and Laboratoire d'Utilisation du Rayonnement Electromagnétique, Université Paris Sud, Bat 209 D, 91405 Orsay Cedex, France

Received July 18, 1997[⊗]

$[Cu(hyetrz)_3](ClO_4)_2 \cdot 3H_2O$ (hyetrz = 4-(2-hydroxyethyl)-1,2,4-triazole) represents the first structurally characterized metal(II) chain compound containing triple N^1,N^2-1,2,4-triazole bridges. The structure has been solved at 298 K by single-crystal X-ray analysis. *catena*-Poly[μ-tris(4-(2-hydroxyethyl)-1,2,4-triazole-N^1,N^2)copper(II)] diperchlorate trihydrate ($C_{12}H_{27}N_9Cl_2O_{14}Cu$) crystallizes in the monoclinic space group $P2_1/n$, $a = 13.877(3)$ Å, $b = 23.023(5)$ Å, $c = 15.351(2)$ Å, $\beta = 91.10(2)°$, $Z = 8$ (Cu(II) units). The Cu(II) ions are linked by triple N^1,N^2-1,2,4-triazole bridges yielding a slightly alternating chain with Cu1−Cu2 = 3.853(2) Å and Cu2−Cu3 = 3.829(2) Å. The EXAFS results are consistent with the crystal structure. At 30 K, the EXAFS signature of the multiple scattering path Cu1−Cu2−Cu3 is clearly observed, confirming that such exceptional long distance EXAFS signals can be used to detect metal alignments in inorganic long chains when crystal structures are not available. The thermal behavior of this multiple scattering signal was compared to those of similar Fe(II) low-spin compounds, and the observed differences have been discussed by comparing their electronic (dynamic Jahn−Teller effect) and vibrational properties. The Cu(II) ions are weakly antiferromagnetically coupled with $J = -1.18(2)$ cm^{-1} (based on the Hamiltonian, $\mathbf{H} = -J[\sum_i \mathbf{S}_i \cdot \mathbf{S}_{i+1}]$). The nature and the magnitude of the antiferromagnetic exchange have been discussed on the basis of the structural features.

Introduction

Polynuclear coordination compounds containing derivatives of 1,2,4-triazole have been of great and increasing interest during the last decade. Several studies have dealt with the search for magneto−structural correlations for transition metal(II) compounds containing N^1,N^2-1,2,4-triazole bridges.[1−9] On the other hand, polynuclear iron(II) 1,2,4-triazole compounds have been found to yield spin-crossover materials exhibiting cooperative behavior.[10−22]

[†] Institut de Chimie de la Matière Condensée de Bordeaux.
[‡] Instituto di Ricerca per lo Sviluppo di Metodologie Cristallografiche CNR.
[§] Université Paris XII-Val de Marne.
[||] Université Paris Sud.
[⊗] Abstract published in *Advance ACS Abstracts,* December 15, 1997.

(1) Prins, R.; Birker, P. J. M. W. L.; Haasnoot, J. G.; Verschoor, G. C.; Reedijk, J. *Inorg. Chem.* **1985**, *24*, 4128.
(2) Bencini, A.; Gatteschi, D.; Zanchini, C.; Haasnoot, J. G.; Prins, R.; Reedijk, J. *Inorg. Chem.* **1985**, *24*, 2812.
(3) Koomen-van Oudenniel, W. M. E.; de Graaff, R. A. G.; Haasnoot, J. G.; Prins, R.; Reedijk, J. *Inorg. Chem.* **1989**, *28*, 1128.
(4) van Koningsbruggen, P. J.; Haasnoot, J. G.; de Graaff, R. A. G.; Reedijk, J.; Slingerland, S. *Acta Crystallogr.* **1992**, *C48*, 1923.
(5) Slangen, P. M.; van Koningsbruggen, P. J.; Goubitz, K.; Haasnoot, J. G.; Reedijk, J. *Inorg. Chem.* **1994**, *33*, 1121.
(6) Slangen, P. M.; van Koningsbruggen, P. J.; Haasnoot, J. G.; Jansen, J.; Gorter, S.; Reedijk, J.; Kooijman, H.; Smeets, W. J. J.; Spek, A. L. *Inorg. Chim. Acta* **1993**, *212*, 289.
(7) van Koningsbruggen, P. J.; Haasnoot, J. G.; Kooijman, H.; Reedijk, J.; Spek, A. L. *Inorg. Chem.* **1997**, *36*, 2487.
(8) van Koningsbruggen, P. J.; Haasnoot, J. G.; Kooijman, H.; Reedijk, J.; Spek, A. L. Manuscript in preparation.
(9) van Koningsbruggen, P. J.; Gluth, M. W.; Ksenofontov, V.; Walcher, W.; Schollmeyer, D.; Levchenko, G.; Gütlich, P. *Inorg. Chim. Acta*, in press.
(10) Kahn, O. *Molecular Magnetism*; VCH Publishers: New York, 1993.
(11) Kahn, O.; Codjovi, E.; Garcia, Y.; van Koningsbruggen, P. J.; Lapouyade, R.; Sommier, L. In *Molecule-Based Magnetic Materials*; Turnbull, M. M., Sugimoto, T., Thompson, L. K., Eds.; ACS Symposium Series No. 644; American Chemical Society: Washington, DC, 1996; p 298.
(12) Kahn, O.; Kröber, J.; Jay, C. *Adv. Mater*. **1992**, *4*, 718.
(13) Jay, C.; Grolière, F.; Kahn, O.; Kröber, J. *Mol. Cryst. Liq. Cryst.* **1993**, *234*, 255.
(14) Kröber, J.; Audière, J.-P.; Claude, R.; Codjovi, E.; Kahn, O.; Haasnoot, J. G.; Grolière, F.; Jay, C.; Bousseksou, A.; Linarès, J.; Varret, F.; Gonthier-Vassal, A. *Chem. Mater*. **1994**, *6*, 1404.
(15) Kröber, J.; Codjovi, E.; Kahn, O.; Grolière, F.; Jay, C. *J. Am. Chem. Soc*. **1993**, *115*, 9810.
(16) Lavrenova, L. G.; Ikorskii, V. N.; Varnek, V. A.; Oglezneva, I. M.; Larionov, S. V. *Koord. Khim*. **1986**, *12*, 207.
(17) Lavrenova, L. G.; Ikorskii, V. N.; Varnek, V. A.; Oglezneva, I. M.; Larionov, S. V. *J. Struct. Chem*. **1993**, *34*, 960.
(18) Lavrenova, L. G.; Ikorskii, V. N.; Varnek, V. A.; Oglezneva, I. M.; Larionov, S. V. *Koord. Khim*. **1990**, *16*, 654.
(19) Lavrenova, L. G.; Yudina, N. G.; Ikorskii, V. N.; Varnek, V. A.; Oglezneva, I. M.; Larionov, S. V. *Polyhedron* **1995**, *14*, 1333.
(20) Haasnoot, J. G. in *Magnetism: A Supramolecular Function*; Kahn, O., Ed.; Kluwer Academic Publishers: Dordrecht, The Netherlands, 1996; p 299.
(21) Garcia, Y.; van Koningsbruggen, P. J.; Codjovi, E.; Lapouyade, R.; Kahn, O.; Rabardel, L. *J. Mater. Chem*. **1997**, *7*, 857.

S0020-1669(97)00895-1 CCC: $14.00

In order to acquire a more detailed understanding about the propagation of the magnetic superexchange *via* diatomic N−N bridges, the structures and magnetic properties of doubly N^1,N^2-1,2,4-triazole-bridged binuclear copper(II) compounds have been investigated.[1−8] These compounds contain polyfunctional 1,2,4-triazole derivatives with N-donating substituents forming five-membered chelate rings.[1−8] The copper(II) ions are linked in the equatorial coordination plane by two N^1,N^2-bridging 1,2,4-triazole ligands. For this class of compounds magneto-structural correlations could be established for the first time.[5,8] In these compounds, the magnetic exchange is propagated *via* the d($x^2 - y^2$) orbitals on the Cu(II) ions which interact with the σ orbitals of the nitrogen atoms of the bridging ligand. It has been experimentally found that the maximal value for the isotropic interaction parameter J is attained when the 1,2,4-triazole ligands link the Cu(II) ions in the most symmetrical way, allowing the N−Cu−N angles to be close to 90°. An increase in these N−Cu−N angles, which is in most cases accompanied by asymmetric bridging of the μ-N^1,N^2-1,2,4-triazole ligands, leads to a decrease in J. Therefore, the dependence of the J value on the structural parameters has a certain similarity with the relation found by Hatfield and Hodgson for planar dihydroxo-bridged copper(II) compounds.[23]

A continuation of this research would be to investigate the propagation of the isotropic exchange *via* triple N^1,N^2-1,2,4-triazole bridges. Linkages of this kind have already been reported mostly for binuclear[24−26] and trinuclear[27−32] compounds of various transition metal(II) ions. Among the copper(II) systems, the linear trinuclear compound $[Cu_3(metz)_6(H_2O)_4](CF_3SO_3)_6(H_2O)_4$ (metz = 3-methyl-4-ethyl-1,2,4-triazole) has been structurally characterized; however, the magnetic data could not be interpreted in a satisfactorily way.[29] Furthermore, a nondetailed X-ray crystallographic study has been reported for the linear chain compound $[Cu(4\text{-amino-}1,2,4\text{-triazole})_3](ClO_4)_2 \cdot 0.5H_2O$.[33]

This paper deals with the synthesis and the first detailed structural and magnetic study of a linear copper(II) chain containing triple N^1,N^2-1,2,4-triazole bridges of the ligand 4-(2-hydroxyethyl)-1,2,4-triazole (abbreviated as hyetrz). We also would like to emphasize that this study is of particular interest in view of the peculiar Fe(II) spin-crossover behavior of an Fe(II) analogue. In fact, we recently reported on $[Fe(hyetrz)_3](3\text{-nitrophenylsulfonate})_2 \cdot 3H_2O$, which shows nonclassical Fe(II) spin-crossover behavior leading to an unprecedented extremely large apparent thermal hysteresis of 270 K.[21] The possibility of application of this material in displays is currently being investigated. Moreover, our efforts are also directed toward an extended characterization of this type of material. Unfortunately, it has not yet been possible to grow single crystals of the Fe(II) derivatives and to elucidate their structures, thus EXAFS was the only method available to directly probe the local structure centered around the metal ion. The possibility to detect metal alignment in these compounds by the multliple scattering EXAFS signal displayed at the double metal−metal distance has been largely discussed.[34,35] However, up to now it was impossible to give any confirmation of our structural interpretation by comparing the results obtained on the Fe(II) derivatives with the EXAFS spectrum of a model compound with a known crystal structure similar to the model assumed for Fe(II). A second point that was still not solved was the reason why the multiple-scattering signal was undoubtedly observed only in the Fe(II) low-spin state and was strongly smeared out in the high-spin state. Two models have been proposed to explain this behavior. One model involves an important structural change, a transition from aligned metallic ions to a zig-zag configuration. The second model assumes that the alignment remains with a significant increase of the amplitude of the vibrational modes. The structural characterization of the present related copper(II) compound with the ligand hyetrz and the comparison of this structure with those of the Fe(II) spin-crossover derivatives may provide more information on these fascinating linear chain compounds.

Experimental Section

Physical Measurements. Elemental analyses were performed by the Service Central d'Analyse (CNRS) in Vernaison, France. Magnetic susceptibilities were carried out in the temperature range 300−2 K on a quantum design MPMS-5S SQUID magnetometer. Magnetic data were corrected for diamagnetic contributions, which were estimated from the Pascal constants and were fitted to theoretical expressions by means of a Simplex routine, with the use of a computer program written by R. Prins.[3] All parameters (J, g) were varied independently during the fitting procedure. This routine minimizes the function $R = |\sum|\chi_{obs} - \chi_{calc}|^2/|\sum|\chi_{obs}|^2|^{1/2}$.

Starting Materials. Commercially available solvents, monoformyl hydrazine, triethyl orthoformate, 2-ethanolamine, and copper(II) perchlorate hexahydrate were used without further purification.

Synthesis of 4-(2-Hydroxyethyl)-1,2,4-triazole (hyetrz). The ligand hyetrz has been prepared from monoformyl hydrazine, triethyl orthoformate and 2-ethanolamine according to the general method described by Bayer et al.[36] Yield: 72%. Mp: 86 °C. ^{1}H NMR (200 MHz) (D_2O): 3.85 (t, CH_2), 4.23 (t, CH_2), 8.50 (s, trz-H). Anal. Calcd for $C_4H_7N_3O$: C, 42.46; H, 6.24; N, 37.16; O, 14.15. Found: C, 44.77; H, 6.41; N, 36.57; O, 14.52.

Synthesis of $[Cu(hyetrz)_3](ClO_4)_2 \cdot 3H_2O$. $Cu(ClO_4)_2 \cdot 6H_2O$ (0.73 mmol, 0.27 g) in 5 mL of water was added to 2.2 mmol (0.25 g) of hyetrz dissolved in 5 mL of water. The solution was filtered, and after a couple of days, the blue compound crystallized upon slow evaporation of the solvent at room temperature. Crystals were washed with water and dried under vacuum. Yield: 60%. Anal. Calcd for $C_{12}H_{27}N_9O_{14}Cl_2Cu$: C, 21.98; H, 4.15; N, 19.22; O, 34.15; Cl, 10.81; Cu, 9.69. Found: C, 21.96; H, 4.38; N, 18.29; O, 33.67; Cl, 10.98; Cu, 9.60.

(22) van Koningsbruggen, P. J.; Garcia, Y.; Codjovi, E.; Lapouyade, R.; Fournès, L.; Kahn, O.; Rabardel, L. *J. Mater. Chem.* **1997**, *7*, 2069.
(23) Crawford, V. H.; Richardson, H. W.; Wasson, J. R.; Hodgson, D. J.; Hatfield, W. E. *Inorg. Chem.* **1976**, *15*, 2107.
(24) Engelfriet, D. W.; Verschoor, G. C.; den Brinker, W. *Acta Crystallogr.* **1980**, *B36*, 1554.
(25) Engelfriet, D. W.; Verschoor, G. C.; Vermin, W. J. *Acta Crystallogr.* **1979**, *B35*, 2927.
(26) Vos, G.; de Kok, A. J.; Verschoor, G. C. *Z. Naturforsch.* **1981**, *36b*, 809.
(27) Antolini, L.; Fabretti, A. C.; Gatteschi, D.; Giusti, A.; Sessoli, R. *Inorg. Chem.* **1991**, *30*, 4858.
(28) (a) Vos, G.; Le Fêbre, R. A.; de Graaff, R. A. G.; Haasnoot, J. G.; Reedijk, J. *J. Am. Chem. Soc.* **1983**, 105, 1682. (b) Vos, G.; de Graaff, R. A. G.; Haasnoot, J. G.; van der Kraan, A. M.; de Vaal P.; Reedijk , J. *Inorg.Chem.* **1984**, *23*, 2905.
(29) (a) Vreugdenhil, W.; Haasnoot, J. G.; Reedijk, J.; Wood, J. S. *Inorg. Chim. Acta* **1990**, *167*, 109. (b) Vreugdenhil, W. Ph.D. Thesis, Leiden University, 1987.
(30) Kolnaar, J. J. A.; van Dijk, G.; Kooijman, H.; Spek, A. L.; Ksenofontov, V. G.; Gütlich, P.; Haasnoot, J. G.; Reedijk, J. *Inorg. Chem.* **1997**, *36*, 2433.
(31) van Koningsbruggen, P. J.; Haasnoot, J. G.; Vreugdenhil, W.; Reedijk, J.; Kahn, O. *Inorg. Chim. Acta* **1995**, *239*, 5.
(32) Thomann, M.; Kahn, O.; Guilhem, J.; Varret, F. *Inorg. Chem.* **1994**, *33*, 6029.
(33) Sinditskii, V. P.; Sokol, V. I.; Fogel'zang, A. E.; Dutov, M. D.; Serushkin, V. V.; Porai-Koshits, M. A.; Svetlov, B. S. *Russ. J. Inorg. Chem.* **1987**, *32*, 1149.
(34) Michalowicz, A.; Moscovici, J.; Ducourant, B.; Cracco, D.; Kahn, O. *Chem. Mater.* **1995**, *7*, 1833.
(35) Michalowicz, A.; Moscovici, J.; Kahn, O. *J. Phys. IV* **1997**, *7*, 633.
(36) Bayer, H. O.; Cook, R. S.; von Meyer, W. C. *U.S. Patent 3, 821, 376*, June 28, 1974.

Table 1. Crystallographic Data for $[Cu(hyetrz)_3](ClO_4)_2 \cdot 3H_2O$

formula	$C_{12}H_{27}Cl_2O_{14}CuN_9$
mol wt	655.8
temp (K)	298
space group	$P2_1/n$ (No. 14)
a (Å)	13.877(3)
b (Å)	23.023(5)
c (Å)	15.351(2)
β (deg)	91.10(2)
V (Å^3)	4904(2)
Z	8
ρ_{calc} (g/cm^3)	1.728
ρ_{obs} (g/cm^3)	1.75
μ (Mo Kα, cm^{-1})	1.227
R(F)[a]	0.068
wR(F)^2 [a]	0.122.

[a] $R(F) = \sum||F_o| - |F_c||/\sum|F_o|$ for $F_o > 4\sigma(F_o)$, $wR(F^2) = [\sum w(F_o^2 - F_c^2)^2/\sum wF_o^2]^{1/2}$, $w = 1/(\sigma^2(F_o^2) + 0.035F^2)$, $F = (F_o + 2F_c)/3$.

Crystallographic Data Collection and Structure Determination. A blue, needle-shaped single crystal with dimensions of 0.12 × 0.15 × 0.78 mm was analyzed by an Enraf-Nonius CAD4 diffractometer using the monochromated Mo Kα X-ray radiation (λ = 0.7069 Å). Accurate unit-cell parameters were obtained by least-squares refinement from 25 centered reflections in the range $10.3° \le \theta \le 22°$. Crystal data and details of data collection and refinement are given in Table 1. The intensities of three standard reflections monitored every 2 h revealed no significant decay over the course of data collection. A semiempirical correction of absorption, based on Ψ scans of three axial reflections, was applied.[37] The structure was solved by direct methods with the program SIR92.[38] Structure refinement based on F^2 was carried out by extended block-diagonal matrix methods, each block being constituted by a chemical entity as Cu, hyetrz, ClO_4, H_2O. Locations of the hydrogen atoms which can be predicted were generated geometrically (C−H = 1.0 Å) and included in the refinement with an isotropic fixed thermal parameter. All non-hydrogen atoms were refined with anisotropic thermal parameters. The high values of the thermal parameters for the perchlorate oxygen atoms and the hydroxy groups suggest disordered positions for these entities. Final reliability factors converged to $R(F) = 0.068$ and $wR(F^2) = 0.122$. Neutral atom scattering factors and anomalous dispersion corrections were taken from the *International Tables for Crystallography*.[39] A final difference Fourier map showed residual density of 1.53 e Å^{-3} near Cu locations and less than ±0.64 e Å^{-3} in the other zones. Final positional parameters are listed in Table 2. Illustrations were produced with *CRYSTAL MAKER*.[40] The calculations were carried out using programs written or modified locally.

EXAFS Data Collection and Analysis. The EXAFS spectra were recorded at LURE, the French synchrotron radiation facility, on the storage ring DCI (1.85 GeV, 300 mA) on the EXAFS13 spectrometer, with a Si331 channel-cut monochromator. The detectors were low pressure (≈0.2 atm) air-filled ionization chambers. Each spectrum is the sum of four recordings in the range 8940−9940 eV, including the copper K-edge (∼8990 eV). The spectra were recorded at room temperature and at 30 K with a liquid helium cryostat. The samples were prepared as homogenous compressed pellets with a mass calculated in order to obtain an absorption jump at the edge $\Delta\mu x \approx 1.5$ with a total absorption above the edge less than $\mu x \approx 2$.

The EXAFS data analysis was performed with the EXAFS pour le MAC programs[41] on an Apple Macintosh personal computer. This

(37) North, A. C. T.; Phillips, D. C.; Mathew, F. S. *Acta Crystallogr.* **1968**, *A24*, 351.
(38) Altomare, A.; Cascarano, G.; Giacovazzo, C.; Guagliardi, A.; Burla, M. C.; Polidori, G.; Camalli, M. *J. Appl. Crystallogr.* **1994**, *27*, 435.
(39) *International Tables for X-ray Crystallography*; Kynoch Press: Birmingham (Present distributor D. Reidel, Dordrecht, The Netherlands), 1974; Vol. IV.
(40) Palmer, D. *Crystal Maker*; Cambridge University Technical Services Ltd.: Cambridge, U.K., 1996.
(41) Michalowicz, A. In *Logiciels pour la Chimie (Software for Chemistry)*; Société Française de Chimie: Paris, 1991; p 102.

Table 2. Final Coordinates and Equivalent Isotropic Thermal Parameters (Å^2) of the Non-Hydrogen Atoms for $[Cu(hyetrz)_3](ClO_4)_2 \cdot 3H_2O$ (Esd's in Parentheses)

	x/a	*y/b*	*z/c*	U_{eq}[a]
Cu(1)	0.5000	0.5000	0.5000	0.0275(3)
Cu(2)	0.48847(4)	0.49905(5)	0.24903(4)	0.0267(2)
Cu(3)	0.5000	0.5000	0.0000	0.0276(3)
N(11)	0.6164(4)	0.5348(3)	0.3984(3)	0.043(3)
N(12)	0.5873(4)	0.5471(3)	0.3145(3)	0.036(3)
C(13)	0.6505(5)	0.5823(3)	0.2809(4)	0.043(3)
N(14)	0.7207(4)	0.5947(3)	0.3401(4)	0.045(3)
C(15)	0.6964(6)	0.5651(5)	0.4109(5)	0.056(4)
C(16)	0.8044(6)	0.6326(5)	0.3280(7)	0.063(5)
C(17)	0.8681(9)	0.6126(8)	0.258(1)	0.098(9)
O(18)	0.816(1)	0.616(1)	0.1782(8)	0.17(1)
N(21)	0.4948(4)	0.4236(3)	0.4374(3)	0.035(2)
N(22)	0.4959(4)	0.4196(3)	0.3482(3)	0.033(2)
C(23)	0.4881(6)	0.3646(3)	0.3291(5)	0.042(3)
N(24)	0.4814(5)	0.3320(3)	0.4034(4)	0.043(3)
C(25)	0.4856(5)	0.3708(3)	0.4686(5)	0.041(3)
C(26)	0.4725(8)	0.2683(4)	0.4098(7)	0.063(5)
C(27)	0.565(1)	0.2377(6)	0.413(2)	0.13(1)
O(28)	0.627(1)	0.2544(9)	0.352(1)	0.17(1)
N(31)	0.3921(3)	0.5320(3)	0.4183(3)	0.033(3)
N(32)	0.3815(3)	0.5282(3)	0.3283(3)	0.031(2)
C(33)	0.2977(5)	0.5510(4)	0.3083(4)	0.041(3)
N(34)	0.2533(4)	0.5707(3)	0.3798(4)	0.042(3)
C(35)	0.3141(5)	0.5570(3)	0.4460(4)	0.041(3)
C(36)	0.1584(6)	0.5990(6)	0.3853(7)	0.073(6)
C(37)	0.0808(9)	0.560(1)	0.412(2)	0.13(1)
O(38)	0.101(1)	0.5335(9)	0.495(1)	0.15(1)
N(41)	0.6264(4)	0.4801(3)	0.1016(3)	0.042(3)
N(42)	0.6022(4)	0.4639(2)	0.1845(3)	0.033(2)
C(43)	0.6751(5)	0.4356(4)	0.2196(5)	0.048(4)
N(44)	0.7457(5)	0.4328(4)	0.1625(5)	0.056(4)
C(45)	0.7131(5)	0.4597(5)	0.0914(5)	0.054(4)
C(46)	0.8415(7)	0.4043(7)	0.1774(8)	0.093(8)
C(47)	0.9065(7)	0.443(1)	0.225(1)	0.12(1)
O(48)	0.869(1)	0.4659(8)	0.305(1)	0.13(1)
N(51)	0.4685(4)	0.5732(3)	0.0630(3)	0.035(2)
N(52)	0.4651(4)	0.5776(3)	0.1519(3)	0.034(2)
C(53)	0.4345(6)	0.6302(4)	0.1683(5)	0.049(4)
N(54)	0.4186(5)	0.6600(3)	0.0932(5)	0.049(3)
C(55)	0.4399(6)	0.6234(4)	0.0293(5)	0.050(4)
C(56)	0.3793(8)	0.7188(4)	0.084(1)	0.076(6)
C(57)	0.283(1)	0.7192(8)	0.049(2)	0.12(1)
O(58)	0.277(1)	0.6923(9)	−0.035(1)	0.16(1)
N(61)	0.4055(4)	0.4537(3)	0.0789(3)	0.033(2)
N(62)	0.3951(3)	0.4570(3)	0.1677(3)	0.030(2)
C(63)	0.3201(5)	0.4241(4)	0.1866(4)	0.041(3)
N(64)	0.2829(4)	0.3998(3)	0.1126(4)	0.040(3)
C(65)	0.3374(5)	0.4202(3)	0.0472(4)	0.037(3)
C(66)	0.1978(6)	0.3624(4)	0.1027(6)	0.052(4)
C(67)	0.1123(6)	0.3952(5)	0.0733(7)	0.065(5)
O(68)	0.1278(5)	0.4185(5)	−0.0095(5)	0.077(4)
Cl(70)	0.1175(2)	0.5722(2)	0.1084(2)	0.060(1)
O(71)	0.2146(6)	0.5572(6)	0.1120(6)	0.102(6)
O(72)	0.0766(9)	0.5447(7)	0.0335(9)	0.124(9)
O(73)	0.079(1)	0.550(1)	0.182(1)	0.18(2)
O(74)	0.102(1)	0.6309(8)	0.105(2)	0.18(2)
Cl(75)	0.1709(3)	0.3863(2)	0.3794(2)	0.087(2)
O(76)	0.180(3)	0.446(1)	0.363(2)	0.25(3)
O(77)	0.122(1)	0.3777(8)	0.4550(9)	0.14(1)
O(78)	0.123(1)	0.3604(8)	0.314(1)	0.14(1)
O(79)	0.265(1)	0.366(1)	0.388(1)	0.19(2)
Cl(80)	0.4401(5)	0.2580(2)	0.1307(3)	0.096(3)
O(81)	0.475(1)	0.3142(5)	0.1366(9)	0.123(9)
O(82)	0.513(2)	0.2173(8)	0.120(2)	0.18(2)
O(83)	0.382(2)	0.255(1)	0.057(1)	0.17(2)
O(84)	0.387(1)	0.247(1)	0.203(1)	0.18(2)
Cl(85)	0.5585(5)	0.7420(2)	0.3259(3)	0.102(3)
O(86)	0.503(1)	0.6929(8)	0.348(1)	0.15(1)
O(87)	0.532(2)	0.7906(7)	0.374(2)	0.17(2)
O(88)	0.545(2)	0.753(1)	0.240(1)	0.19(2)
O(89)	0.653(2)	0.728(1)	0.347(2)	0.24(3)
O(91)	0.7227(7)	0.3595(5)	0.3911(6)	0.085(5)
O(92)	0.337(2)	0.317(1)	−0.094(1)	0.20(2)
O(93)	−0.079(1)	0.339(1)	0.389(1)	0.19(2)

[a] U_{eq} = $^1/_3$ of the trace of the orthogonalized **U**, with $\mathbf{U} = \sum_i\sum_j U_{ij} a_i^* a_j^* a_i a_j$.

standard EXAFS analysis[42] includes linear pre-edge background removal, polynomial and cubic spline atomic absorption calculation, Lengeler−Eisenberger EXAFS spectra normalization,[43] and reduction from the absorption data $\mu(E)$ to the EXAFS spectrum $\chi(k)$ with $k = \sqrt{[(2m_e)/\tilde{n}h^2)](E - E_o)}$ where E_o is the energy threshold taken at the absorption maximum (8993 eV). Radial distribution functions $F(R)$ were calculated by Fourier transforms of $k^3w(k)\chi(k)$ in the range 2−14 Å^{-1}, where $w(k)$ is a Kaiser−Bessel apodization window with a smoothness coefficient $\tau = 2.5$. After Fourier filtering, the first single-shell Cu − 6*N* was fitted in the range 3−13 Å^{-1} to the standard EXAFS formula, without multiple scattering

$$k\chi(k) = -S_o^2 \sum \left[\frac{N}{R^2} |f(\pi,k)| e^{-2\sigma^2 k^2} e^{-(2R/\lambda(k))} \sin(2kR + 2\partial_1(k) + \psi(k)) \right]$$

S_o^2 is the inelastic reduction factor; N is the number of nitrogen atoms at the distance R from the copper center; $\lambda(k) = k/\Gamma$ is the mean-free path of the photoelectron, with $\Gamma = 1$ Å^{-2} in our fits; σ is the Debye−Waller coefficient, characteristic of the width of the Cu−N distance distribution; $\partial_1(k)$ is the central atom phase shift; $|f(\pi,k)|$ and $\psi(k)$ are the amplitude and phase of the nitrogen backscattering factor. We used the spherical-waves theoretical amplitudes and phase shifts calculated by the code FEFF.[44] Since we use theoretical phase shifts, it is necessary to fit the energy threshold E_o by adding an extra fitting parameter ΔE_o. The Cu site is strongly distorted, so that it was necessary to introduce two Cu−N distances at 2 and 2.36 Å. This is why the EXAFS is represented by a sum of two terms.

The goodness of fit is given by $\rho(\%) = \{[k\chi_{exp}(k) - k\chi_{th}(k)]^2\}/\Sigma\{k\chi_{exp}(k)]^2\}$. We have estimated the significance of the two-shell model improvement, compared with a fit assuming only one average distance, by using the standard statistical *F*-test described for EXAFS fittings by Freund.[45] The fit is performed on a filtered spectrum containing N_{ind} independent points, with $N_{ind} = (2\Delta R\Delta k/\pi + 2)$ where ΔR (Å) is the width of the filtered Fourier peak and Δk (Å^{-1}) the spectral width. In order to test if the fit is actually improved by increasing the number of parameters from n_1 to n_2, one must calculate $F = (\rho_1 - \rho_2)(N_{ind} - n_2)/[\rho_2(n_2 - n_1)]$, where ρ_1 and ρ_2 are the two fitting residuals. Actually, the F value should be evaluated with the use of the two statistical χ^2, but if the average experimental error bars are the same for the two models, they cancel and the use of ρ instead of χ^2 is relevant. The values of F, n_1, n_2, and N_{ind} were used to calculate the F statistics[46] and estimate the probability that increasing the number of parameters leads to a statistically significant improvement.

Since the crystal structure of the compound studied is known, the fit of the EXAFS spectrum of the first coordination shell is used only as a consistency test. The interesting part of this EXAFS study is the modeling of the whole spectrum by an ab-initio calculation using all the atoms lying around the central copper(II) ion within a sphere of 8 Å, in order to include at least two shells of copper neighbors. This theoretical calculation was performed with the ab-initio modeling program from Rehr[44] FEFF7.

(42) (a) Teo, B. K. in *Inorganic Chemistry Concepts, EXAFS: Basic Priciples and Data Analysis*; Springer-Verlag: Berlin, 1986; p 9. (b) Königsberger, D. C.; Prins, R. *X-Ray Absorption Principles, Applications, Techniques of EXAFS, SEXAFS and XANES*; John Wiley: New York, 1988. (c) Lytle, F. W.; Sayers, D. E.; Stern, E. A., Report of the International Worshop on Standards and Criteria in X-Ray Absorption Spectroscopy. *Physica* **1989**, *B158*, 701.
(43) Lengeler, B.; Eisenberger P. *Phys. Rev.* **1980**, B21, 4507.
(44) (a) Rehr, J. J.; Zabinsky, S. I.; Albers, R. C. *Phys. Rev. Lett.* **1992**, *69*, 3397. (b) Rehr, J. J. *Jpn. J. Appl. Phys.* **1993**, *32*, 8. (c) Rehr, J. J.; Mustre de Léon, J.; Zabinsky, S. I.; Albers, R. C. *J. Am. Chem. Soc.* **1991**, 113, 5135. (d) Mustre de Leon, J.; Rehr, J. J.; Zabinsky, S. I.; Albers, R. C. *Phys. Rev.* **1991**, *B44*, 4146. (e) Rehr, J. J.; Albers, R. C. *Phys. Rev.* **1990**, *B41*, 8139.
(45) Freund, J. *Phys. Lett. A* **1991**, *157*, 256.
(46) (a) Bevington, P. R. in *Data Reduction and Error Analysis for the Physical Sciences*; Mc Graw-Hill: New York, 1969. (b) Press, W. H.; Flanery, B. P.; Teukolsky, S. A.; Vetterling, W. T. In *Numerical Recipes*; Cambridge University Press: Cambridge, U.K., 1986.

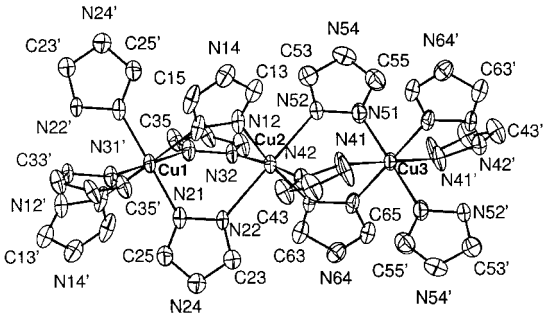

Figure 1. CRYSTAL MAKER[40] drawing and atomic-labeling system showing the structure of $[Cu(hyetrz)_3](ClO_4)_2 \cdot 3H_2O$. Hydroxyethyl groups and hydrogen atoms have been omitted for clarity. Primed atoms are generated by the symmetry operations $1 - x$, $1 - y$, $1 - z$ and $1 - x$, $1 - y$, $-z$.

Table 3. Selected Bond Distances (Å) for $[Cu(hyetrz)_3](ClO_4)_2 \cdot 3H_2O$ (Esd's in Parentheses)

Cu1−N11	2.404(6)	Cu2−N12	2.015(5)
Cu1−N21	2.005(6)	Cu2−N22	2.381(5)
Cu1−N31	2.070(5)	Cu2−N32	2.050(5)
Cu3−N41	2.369(6)	Cu2−N42	2.046(5)
Cu3−N51	1.996(5)	Cu2−N52	2.362(5)
Cu3−N61	2.094(5)	Cu2−N62	2.028(5)

Results

Description of the Structure of $[Cu(hyetrz)_3](ClO_4)_2 \cdot 3H_2O$. A CRYSTAL MAKER[40] projection of the cationic linear copper(II) chain is depicted in Figure 1, whereas relevant bond length and bond angle information is given in Tables 3 and 4. The coordination polymer consists of a crystallographically independent unit comprising two copper(II) ions, Cu1 and Cu3, in special positions and another copper(II) ion in a general position (Cu2) and six symmetry independent hyetrz ligands. The linear chain (see Figure 2a) is generated by the inversion involving the crystallographic centers of symmetry located on Cu1 and Cu3.

Three hyetrz ligands act as bidentate ligands linking the copper(II) ions *via* the nitrogen atoms N1 and N2. All copper(II) ions are in a distorted (4 + 2) octahedral environment formed by six N-donating hyetrz ligands. The basal plane is formed by four nitrogen donor atoms at 1.996(5)−2.094(5) Å, whereas two hyetrz ligands coordinate axially at significantly longer distances (2.369(6)−2.404(6) Å). Structural data have been obtained for the related linear chain compound $[Cu(4\text{-amino-}1,2,4\text{-triazole})_3](ClO_4)_2 \cdot 0.5H_2O$.[33] It appears that the crystallographic symmetry is identical to that of the present compound, however, the distortion of the Cu(II) octahedron is not entirely similar. In that compound, three pairs of Cu−N distances could be distinguished: short, 2.019(3) Å; average, 2.101(3) Å; and long, 2.327(3) Å. The lack of detailed structural data does not allow an extended comparison between this and the present linear Cu(II) chain compound.

All copper(II) ions are not significantly displaced from their equatorial coordination sphere. The least-squares planes through the equatorial planes of the Cu(II) octahedra make angles of 46(1)° for Cu1 and Cu2 and 53(3)° for Cu2 and Cu3.

The three hyetrz ligands linking neighboring Cu(II) ions do not conserve a perfect trigonal symmetry. In contrast, in the linear trinuclear compounds with the related ligand 4-ethyl-1,2,4-triazole, $[M(II)_3(ettrz)_6(H_2O)_6](CF_3SO_3)_6$ (M = Fe (high-spin and low-spin),[28] Mn,[47] and Zn[48]), $C3_2$ symmetry is present.

(47) Spek, A. L.; Vos, G. *Acta Crystallogr*. **1983**, *C39*, 990.
(48) Vos, G.; Haasnoot, J. G.; Verschoor, G. C.; Reedijk, J.; Schaminee, P. E. L. *Inorg. Chim. Acta* **1985**, *105*, 31.

Table 4. Selected Bond Angles (deg) for $[Cu(hyetrz)_3](ClO_4)_2 \cdot 3H_2O$ (Esd's in Parentheses)

N11−Cu1−N21	90.0(2)	N21−Cu1−N31′	89.8(2)
N11−Cu1−N31	88.6(2)	N31−Cu1−N11′	91.4(2)
N11−Cu1−N11′	180.0	N31−Cu1−N21′	89.8(2)
N11−Cu1−N21′	90.0(2)	N31−Cu1−N31′	180.0
N11−Cu1−N31′	91.4(2)	N11'−Cu1−N21′	90.0(2)
N21−Cu1−N31	90.2(2)	N11'−Cu1−N31′	88.6(2)
N21−Cu1−N11′	90.0(2)	N21'−Cu1−N31′	90.2(2)
N21−Cu1−N21′	180.0		
N12−Cu2−N22	94.7(2)	N22−Cu2−N62	92.6(2)
N12−Cu2−N32	91.0(2)	N32−Cu2−N42	172.2(2)
N12−Cu2−N42	86.3(2)	N32−Cu2−N52	91.8(2)
N12−Cu2−N52	88.8(2)	N32−Cu2−N62	93.5(2)
N12−Cu2−N62	171.7(2)	N42−Cu2−N52	95.5(2)
N22−Cu2−N32	84.0(2)	N42−Cu2−N62	90.2(2)
N22−Cu2−N42	88.9(2)	N52−Cu2−N62	84.2(2)
N22−Cu2−N52	174.6(2)		
N41−Cu3−N51	90.6(2)	N51−Cu3−N61″	89.8(2)
N41−Cu3−N61	89.1(2)	N61−Cu3−N41″	90.9(2)
N41−Cu3−N41″	180.0	N61−Cu3−N51″	89.8(2)
N41−Cu3−N51″	89.4(2)	N61−Cu3−N61″	180.0
N41−Cu3−N61″	90.9(2)	N41″−Cu3−N51″	90.6(2)
N51−Cu3−N61	90.2(2)	N41″−Cu3−N61″	89.1(2)
N51−Cu3−N41″	89.4(2)	N51″−Cu3−N61″	90.2(2)
N51−Cu3−N51″	180.0		
Cu1−N11−N12	119.2(4)	Cu1−N21−N22	122.4(4)
Cu1−N11−C15	130.9(5)	Cu1−N21−C25	129.8(5)
Cu2−N12−N11	122.7(4)	Cu2−N22−N21	125.8(4)
Cu2−N12−C13	126.8(5)	Cu2−N22−C23	126.9(5)
Cu1−N31−N32	129.9(4)	Cu3−N41−N42	118.1(4)
Cu1−N31−C35	123.7(5)	Cu3−N41−C45	131.6(5)
Cu2−N32−N31	123.1(4)	Cu2−N42−N41	123.1(4)
Cu2−N32−C33	130.0(5)	Cu2−N42−C43	126.4(5)
Cu3−N51−N52	123.9(4)	Cu3−N61−N62	128.6(4)
Cu3−N51−C55	127.9(5)	Cu3−N61−C65	122.8(4)
Cu2−N52−N51	124.4(4)	Cu2−N62−N61	124.0(4)
Cu2−N52−C53	128.9(5)	Cu2−N62−C63	129.3(5)

[a] Primed atoms are generated by the symmetry operation $1 - x$, $1 - y$, $1 - z$; double primes atoms are generated by $1 - x$, $1 - y$, $-z$.

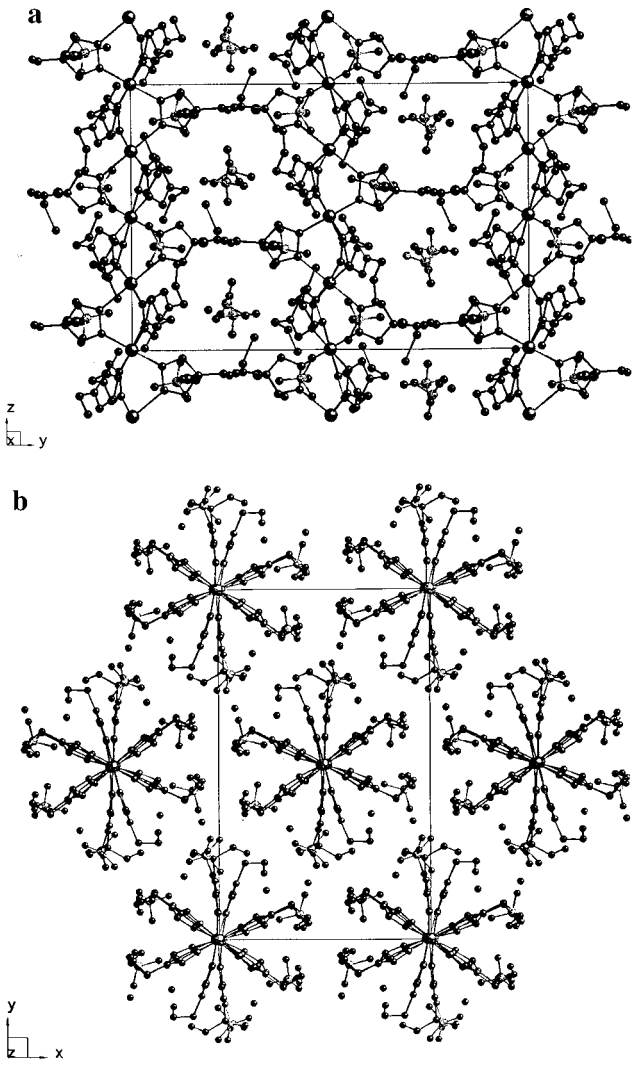

Figure 2. CRYSTAL MAKER[40] drawing showing the structure of $[Cu(hyetrz)_3](ClO_4)_2 \cdot 3H_2O$ (a) along the *a*-axis and (b) along the *c*-axis.

This may be due to important distortions from O_h symmetry about the Cu(II) ions, which is also reflected in, *e.g.*, the Cu−N−N angles as well as the Cu−N−N−Cu torsion angles involving the bridging hyetrz ligands (*vide infra*). All 1,2,4-triazole rings are fairly planar; the deviation from the least-squares plane through the ring atoms is smaller than 0.02(1) Å. The least-squares planes through the hyetrz ligands linking Cu1 and Cu2 are 54(2)° for hyetrz-1 and hyetrz-2, 69(2)° for hyetrz-2 and hyetrz-3, and 64.6(4)° for hyetrz-1 and hyetrz-3. The 3-fold symmetry of the triple hyetrz linkage between Cu2 and Cu3 shows comparable distortions, yielding angles of 50(3)° between hyetrz-4 and hyetrz-5, 71(1)° between hyetrz-5 and hyetrz-6, and 66(3)° between hyetrz-6 and hyetrz-4.

These similar distortions from 3-fold symmetry are also reflected by the strong analogy between the N^1,N^2-1,2,4-triazole bridging modes from Cu1 to Cu2 and from Cu2 to Cu3. Hyetrz-1 links Cu1 and Cu2 with a long distance (Cu1−N11 = 2.404(6) Å) and a rather small angle (Cu1−N11−N12 = 119.2(4)°) involving Cu1, whereas the distance (Cu2−N12 = 2.015(5) Å) and angle (Cu2−N12−N11 = 122.7(4)°) involving Cu2 may be considered as normal. Apparently, the maintaining of these Cu(II) ions under these geometric dispositions requires an extremely large Cu1−N11−N12−Cu2 torsion angle of −37.5(2)°. Also hyetrz-2 shows considerable asymmetry in the bridging mode with respect to the Cu−N bond lengths. As for hyetrz-1, the short distance (Cu1−N21 = 2.005(6) Å) corresponds to a normal Cu1−N21−N22 angle of 122.4(4)°. However, for hyetrz-2, the long Cu2−N22 distance of 2.381(5) Å is now accompanied by a much larger Cu2−N22−N21 angle of 125.8(4)°. In this case, only a torsion angle of −6.4(2)° is required. In contrast, hyetrz-3 links Cu1 and Cu2 with about identical Cu1−N31 = 2.070(5) Å and Cu2−N32 = 2.050(5) Å distances. However, the N^1,N^2-1,2,4-triazole bridging mode shows a rather high degree of asymmetry with respect to the Cu−N−N bond angles, which are Cu1−N31−N32 = 129.9(4)° and Cu2−N32−N31 = 123.1(4)°. The torsion angle Cu1−N31−N32−Cu2 is −10.7(3)°. For the ligands hyetrz-4, -5 and -6 which establish the linkage between Cu2 and Cu3, the same features are observed. The bond distances (±0.04 Å) and bond and torsion angles (±2°) involving hyetrz-4, hyetrz-5, and hyetrz-6 are close to those observed for hyetrz-1, hyetrz-2, and hyetrz-3, respectively.

The minor differences in the bridging geometry of the two pairs of triple μ-N^1,N^2-1,2,4-triazoles are reflected in a slight difference in Cu−Cu separations: Cu1−Cu2 = 3.8530(8) Å, whereas Cu2−Cu3 = 3.8293(2) Å. Cu2 is displaced by 0.162(1) Å from the Cu1−Cu3 axis. Therefore, the chain is only very slightly zig-zagged, which can also be seen from the angle of 175.18(2)° between the vectors through the pairs of Cu(II) ions (Cu1,Cu2) and (Cu2,Cu3).

Clearly, in order to establish the linkage of Cu(II) ions in Jahn−Teller-distorted octahedra by triple μ-N^1,N^2-1,2,4-triazole bridges, the geometrical disposition of the ligands becomes such that important deviations from the ideal 3-fold axis running

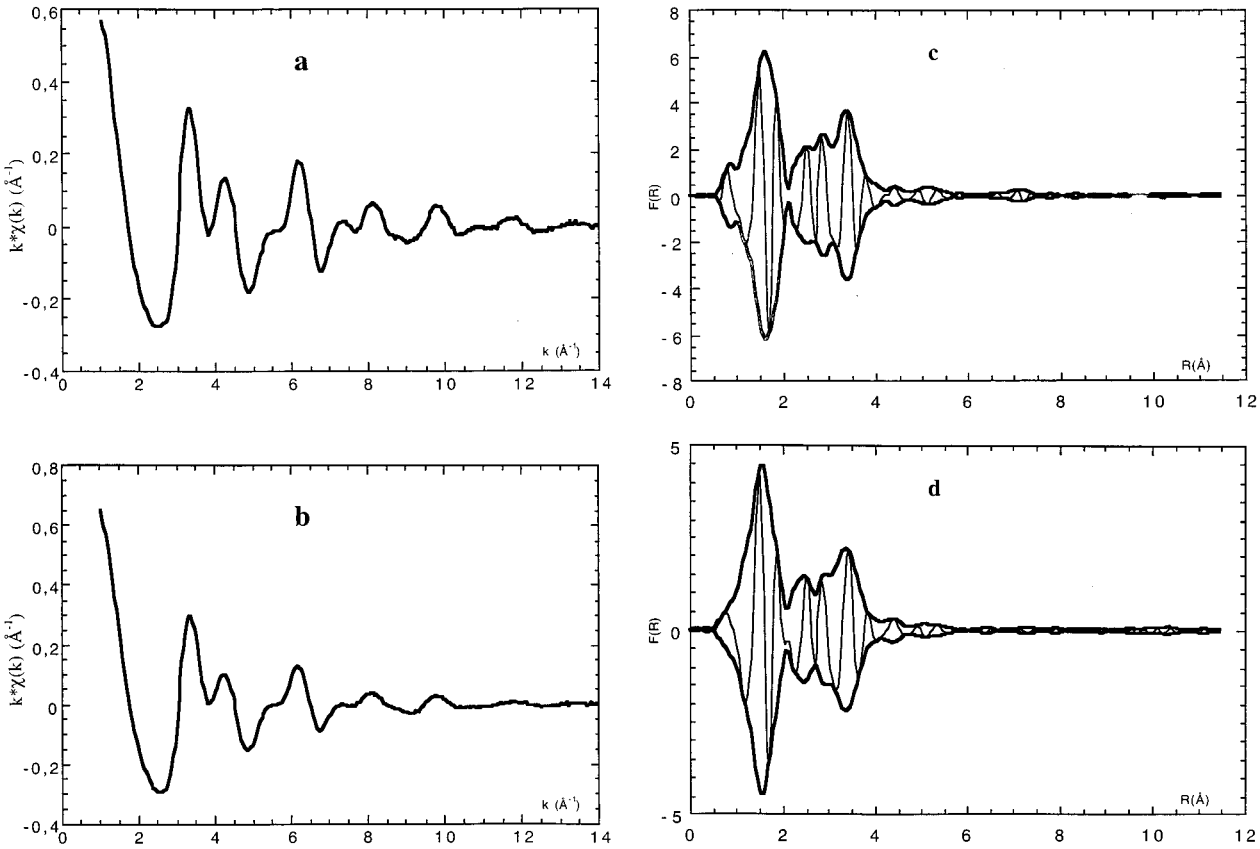

Figure 3. Experimental EXAFS spectra of $[Cu(hyetrz)_3](ClO_4)_2 \cdot 3H_2O$ (a) $k\chi(k)$ spectrum at 30 K (b) $k\chi(k)$ spectrum at 300 K, (c) Fourier transform (± modulus and imaginary part) at 30 K, (d) Fourier transform (± modulus and imaginary part) at 300 K.

through the Cu(II) ions are required. This is illustrated in Figure 2b showing a view of the linear chain structure along the *c*-axis.

It should be noticed that the Cu−Cu distances observed in the present coordination polymer are significantly longer than the 3.719(7) Å for Cu(II) ions linked by triple μ-N^1,N^2-1,2,4-triazole bridges in the linear trinuclear compound $[Cu_3(metz)_6(H_2O)_4](CF_3SO_3)_6(H_2O)_4$ (metz = 3-methyl-4-ethyl-1,2,4-triazole).[29] This is mainly due to the dynamic Jahn−Teller effect involving the central Cu(II) ion, leading to a perfectly symmetric octahedron with six relatively short Cu−N distances of 2.14(5) Å.

Clearly, when one or two μ-N^1,N^2-1,2,4-triazole bridges are replaced by (smaller) monoatomic anions, the Cu−Cu distance tends to shorten even more. For instance, $[Cu(4H\text{-}1,2,4\text{-triazole})Cl_2]_\infty$ has a linear Cu(II) chain structure in which the metal ions are linked by a single μ-N^1,N^2-1,2,4-triazole bridge and two μ-chloride anions yielding a Cu−Cu distance of 3.40 Å.[49] Furthermore, several linear trinuclear copper(II) compounds having double μ-N^1,N^2-1,2,4-triazoles together with a bridging halogen anion have been reported. In $[Cu_3(H_2ahmt)_6Cl_4]Cl_2$ (H_2ahmt = 4-amino-3,5-bis(hydroxymethyl)-1,2,4-triazole), the Cu−Cu distance is 3.5682(5) Å,[50] whereas in $[Cu_3(tmtz)_8F_2](BF_4)_4(H_2O)_2$ (tmtz = 3,4,5-trimethyl-1,2,4-triazole), the Cu−Cu separation is only 3.362(3) Å.[51]

In the present compound, the perchlorate anions are noncoordinating and appear to be involved in extensive hydrogen-bonding interactions with the hydroxy group of the hyetrz ligand, as well as with the lattice water molecules. The strong thermal coefficients associated with the oxygen atoms originating from the ethyl groups, as well as from the water molecules and perchlorate anions, reflect their partial delocalization. Consequently, it is rather difficult to analyze in detail the way these groups are involved in hydrogen-bonding interactions. However, the relatively short oxygen−oxygen contacts listed in Table 5 are indicative of the presence of an extended hydrogen-bonding network. Interestingly, there also appears to be a short O18···O68 ($1-x$, $1-y$, $-z$) contact of 2.83(2) Å. This would imply the occurrence of a hydrogen bond between the hydroxy groups from hyetrz ligands originating from neighboring (*i.e.*, intrachain) triple μ-triazole links. There is no indication for hydrogen-bonding interactions taking place between hydroxyethyl groups of hyetrz ligands originating from different linear Cu(II) chains.

Table 5. Relevant Interatomic Distances (up to 3 Å) for the Hydrogen Bonding Interactions in $[Cu(hyetrz)_3](ClO_4)_2 \cdot 3H_2O$ (Esd's in Parentheses)

O18···O68[a]	2.83(2)
O18···092[a]	2.91(3)
O28···091	2.82(2)
O68···072[b]	2.98(2)
O83···O92	2.78(4)
O88···O93[c]	2.85(3)
O91···O93[d]	2.79(3)

[a] Generated by the symmetry operations $1-x$, $1-y$, $-z$. [b] Generated by the symmetry operation $-x$, $1-y$, $-z$. [c] Generated by the symmetry operation $0.5-x$, $0.5+y$, $0.5-z$. [d] Generated by the symmetry operation $1+x$, y, z.

EXAFS Study. The experimental EXAFS spectra and their Fourier transforms at 30 K and at room temperature are represented in Figure 3. The positions of the principal features are not changed when increasing the temperature: the copper local structure is not dramatically modified. On the other hand, the amplitudes strongly decrease. We interpret this behavior as an important sensitivity of the thermal vibrations when the temperature increases, leading to a temperature-driven increase

(49) Jarvis, J. A. *Acta Crystallogr.* **1962**, *15*, 964.
(50) van Koningsbruggen, P. J.; van Hal, J. W.; de Graaff, R. A. G.; Haasnoot, J. G.; Reedijk, J. *J. Chem. Soc., Dalton Trans.* **1993**, 2163.
(51) Keij, F. S. Ph.D. Thesis, Leiden University, 1990.

Table 6. Fitting[a] of the First Cu Coordination Sphere of the EXAFS Data for $[Cu(hyetrz)_3](ClO_4)_2 \cdot 3H_2O$

	N	σ (Å)	*R* (Å)	ΔE_o (eV)	ρ(%)	*F*, *P*(*F*) (%)
300 K, one Cu−N distance	3.4	0.066	2.01	−8.4	6.6	
300 K, two Cu−N distances	3.71, 0.82	0.072, 0.072	2.00 2.38	−8.9, −8.9	0.9	15.8, 99%
30 K, one Cu−N distance	3.5	0.045	2.02	−6.6	8.7	
30 K, two Cu−N distances	4, 1.5	0.054, 0.054	2.01 2.36	−8.4, −8.4	2.1	7.9, 94%

[a] Γ was taken to 1 Å^{-2} and S_o^2 was found to be 0.94 in order to obtain (4 + 2) nitrogens in the first coordination shell. After Fourier filtering, the data set contains 11 independent points. The fit with only one Cu−N distance involves 4 fitted parameters (*N*, σ, *R*, and ΔE_o), and in the two-shell fit, two parameters are added (*N* and *R* for the long Cu−N distance). In order to limit the total number of fitted parameters, the Debye−Waller factors and energy shifts of the two shells are kept equal during the refinement. The energy shift ΔE_o is relative to the energy of the absorption maximum, 8993 eV.

of the thermal fluctuations of the copper−neighbor distances. The small peak observed at 7 Å on the Fourier transform has almost totally disappeared at 300 K (Figure 3d) but is clearly observed above the noise level at 30 K (Figure 3c).

The fitting results of the first Cu coordination shell are given in Table 6. The two important features of these results are the following: (i) the Cu−N octahedral geometry determined by EXAFS is consistent with the crystal structure. The strong distorsion of the octahedron with four short distances at 2 Å and two long distances at 2.36−2.40 Å is modeled in EXAFS by a two-shell fit which is statistically better than a one-shell model, with an *F* probability greater than 90%. The slight differences between the distances obtained by EXAFS and by crystallography are inside the commonly observed EXAFS error bars (0.02 Å). (ii) The EXAFS signal amplitude of the first shell is quite sensitive to the temperature. The increase of the Debye−Waller factor from 0.05 to 0.07 Å is quite important. One can observe that if the number of neighbors obtained at 30 K is consistent with the actual structure ($N_1 = 4$, $N_2 = 1.5$, assuming $S_o^2 = 0.94$), these numbers are under-evaluated at 300 K, especially for the long distance ligands: N1 = 3.7, N2 = 0.8. This behavior is well-documented in the EXAFS studies of systems with large distributions of distances.[43] The reason is the inadequacy of the harmonic vibration model when the Debye−Waller factor is too large.

The EXAFS signal corresponding to the second shell of atoms (distances between 2.8 and 4 Å, see Figure 3) cannot be treated in the same way as the signal of the first shell. In the latter case, it was possible to filter and fit the simplified EXAFS spectrum by only taking into account single backscattering contributions. However, for the second shell of atoms, the situation is more complicated, since now the EXAFS contributions are strongly overlapping and cannot be separated. Moreover, single backscattering and mutliple scattering terms are mixed together and cannot be treated separately in this range of distances. Therefore, we have preferred to model the complete EXAFS spectrum by an ab-initio treatment with the program FEFF.

The Fourier transform of the ab-initio FEFF model, compared to the experimental spectrum at 30 K, is presented in Figure 4a for the imaginary part and in Figure 4b for the modulus. In order to take into account all the atoms in a sphere involving the second Cu neighbors, *i.e.*, at 7.7 Å from the central Cu(II), it was necessary to use more than 1000 scattering paths. In this treatment, the single and multiple scattering paths of the photoelectrons were considered. To avoid memory overflow, we restricted our calculation to scattering paths of order 2−5, neglecting paths of greater order. A detailed analysis of the output FEFF file shows that the dominant signals are the single scattering paths from the first neighbors (Cu−N distorded octahedron) and single and multiple scattering paths by carbon and nitrogen atoms from the triazole ring, between 3 and 4 Å.

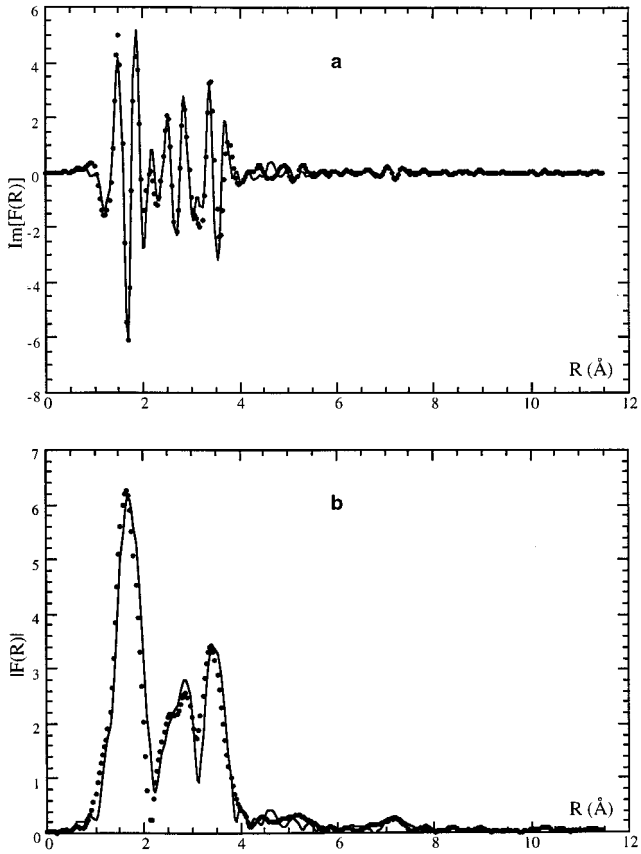

Figure 4. Fourier transforms of the experimental EXAFS spectrum of $[Cu(hyetrz)_3](ClO_4)_2 \cdot 3H_2O$ at 30 K (···) and the FEFF ab-initio model (—): (a) imaginary parts, (b) modulus.

The third Fourier peak amplitude is composed of 70% Cu−Cu single scattering (3.85 Å) and 30% from the multiple scattering by the light atoms (C and N triazole ring). From 4 to 7 Å the EXAFS contibutions are small, if not totally negligible. Finally, the peak around 7 Å is composed mainly by the mutliple scattering paths (order 3 and 4) involving only the copper ions. Prior to any refinement, we compared the peak positions of the FEFF theoretical model and the experimental Fourier transform. Since these positions fitted correctly, it was not necessary to refine the atomic positions. Only the amplitudes needed to be fitted, and this was done by refining the Debye−Waller factors of all the scattering paths. These Debye−Waller factors characterize the thermal vibrations. The complete FEFF input and output are given as supporting information. The most relevant values for the Debye−Waller factors resulting from this FEFF model are gathered in Table 7. In order to test the weight of the Cu contributions to the total signal, we performed FEFF calculations after some structural changes involving these atoms. The double Cu−Cu distance (3 and 4 order multiple scattering paths) disappears almost completely if the Debye-

Table 7. Debye−Waller Factors Obtained in the FEFF Model Refinement (Figure 4)

	σ (Å)
general value for almost all the 1100 scattering paths	0.07
first-coordination sphere. Cu−N octahedron[a]	0.056
Cu−Cu single backscattering path[b]	0.056
Cu−Cu−Cu third- and fourth-order multiple scattering paths[c]	0.08

[a] Single backscattering paths. Distances: 2.01−2.38 Å. [b] Third Fourier transform peak. Distances: 3.82−3.85 Å. [c] Distances: 7.65−7.70 Å.

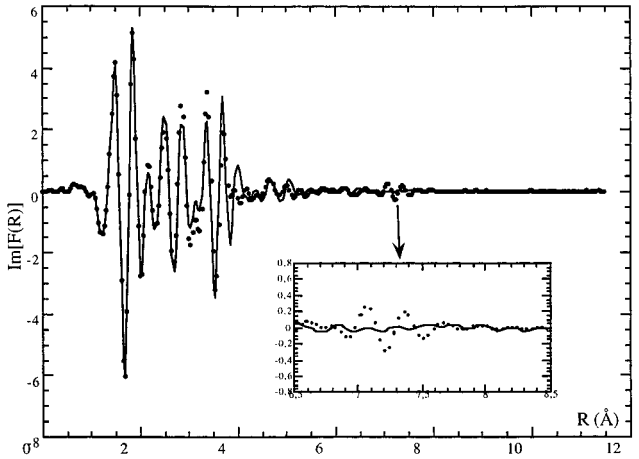

Figure 5. Fourier transforms of the FEFF model of $[Cu(hyetrz)_3](ClO_4)_2 \cdot 3H_2O$, including all the scattering path (···) and the FEFF model reduced to the single backscattering contributions (—). The 6.5−8.5 Å region is zoomed in order to underline the importance of the Cu−Cu−Cu multiple scattering contribution compared to the single scattering.

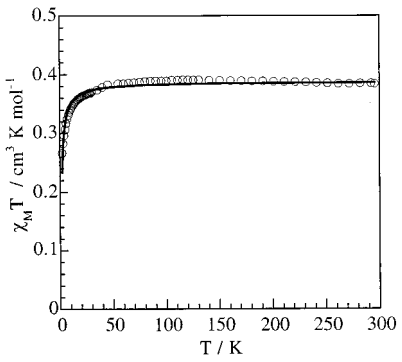

Figure 6. Observed (○) and calculated (—; $J = -1.18(2)$ cm^{-1}, $g = 2.03(1)$) $\chi_M T$ *vs* T curves for $[Cu(hyetrz)_3](ClO_4)_2 \cdot 3H_2O$.

Waller factors σ^2 of these contributions are increased from 0.0065 to 0.0155 Å^2. It is also totally smeared out if we forget the mutliple scattering paths and use only the single scattering ones (Figure 5). The most significant result obtained within this FEFF modeling of the EXAFS spectrum is that the peak around 7 Å is almost exclusively due to the Cu−Cu−Cu multiple scattering signal (order 3 and 4). Furthermore, its amplitude is quite sensitive to a change in the thermal vibration amplitudes.

Magnetic Properties. The magnetic behavior of $[Cu(hyetrz)_3](ClO_4)_2 \cdot 3H_2O$ is shown in Figure 6 in the form of a $\chi_M T$ *vs* T plot, χ_M being the molar magnetic susceptibility per copper(II) ion and T being the temperature. At 290 K, the $\chi_M T$ value is 0.384 cm^3 K mol^{-1}, which is approximately the value expected for a single uncoupled copper(II) ion. The value of $\chi_M T$ decreases upon cooling, reaching a value of 0.265 cm^3 K mol^{-1} at 2 K. This behavior is characteristic for compounds with an overall antiferromagnetic interaction between the metal(II) ions. However, this antiferromagnetic interaction between adjacent copper(II) ions should be very weak, which is also illustrated by the absence of a maximum in the χ_M *vs* T curve above 2 K.

The magnetic data have been interpreted using the expression for the molar magnetic susceptibility of a chain of uniformly spaced copper(II) ions based on the model derived by Bonner and Fisher.[52,53]

$$\chi = \left(\frac{Ng^2\beta^2}{kT}\right)\left(\frac{0.25 + 0.074975x + 0.075235x^2}{1.0 + 0.9931x + 0.172135x^2 + 0.757825x^2}\right) \quad (1)$$

in which $x = |J|/kT$. J is the isotropic interaction parameter occuring in the spin Hamiltonian

$$\mathbf{H} = -J(\sum_i \mathbf{S}_i.\mathbf{S}_{i+1}) \quad (2)$$

The assumption of neglible magnetic exchange between second-neighbor copper(II) ions is justified in view of the study of the triply N^1,N^2-1,2,4-triazole-bridged Fe(II)−Fe(II)−Fe(II)[28] and Co(II)−Co(III)−Co(II)[27] trinuclear clusters, where the central metal ion is diamagnetic, and no magnetic interactions could be detected between the paramagnetic terminal metal ions.

In eq 1, N, g, β, k, and T have their usual meanings. A good fit has been obtained for the parameters $g = 2.03(1)$ and $J = -1.18(2)$ cm^{-1} (see Figure 6). J may be considered as a mean value between $J(1 + \alpha)$ and $J(1 - \alpha)$, where α is a very weak alternation parameter.

Discussion and Conclusion

$[Cu(hyetrz)_3](ClO_4)_2 \cdot 3H_2O$ represents the first structurally characterized linear metal(II) chain containing triple N^1,N^2-1,2,4-triazole bridges. In this compound a relatively small antiferromagnetic interaction ($J = -1.18(2)$ cm^{-1}) has been found between adjacent metal(II) ions. The unpaired electron for the d^9 ion clearly resides in the d($x^2 - y^2$) orbital, with hardly any spin density in the direction of the axially coordinating 1,2,4-triazole ligands. The magnitude of the antiferromagnetic interaction between Cu(II) ions can, therefore, be explained by the superexchange pathway involving the σ orbitals of the N^1,N^2-diazine moiety of the bridging triazole network.[1−9] It should be noted that the d($x^2 - y^2$) orbitals located on the Cu(II) ions are only favorably oriented to yield a significant overlap on the 1,2,4-triazole ligand linking the metal(II) ions with rather short Cu−N distances, *i.e.*, hyetrz-3 between Cu1 and Cu2 and hyetrz-6 between Cu2 and Cu3. Consequently, the main pathway for the superexchange only proceeds through one triazole ligand. However, the bridging geometry of this ligand is very asymmetric and involves one normal (about 123°) and one rather large Cu−N−N angle (130°). Furthermore, the 1,2,4-triazole tends to twist out of the equatorial plane formed by the two Cu(II) ions involved, which is illustrated by the torsion angle of about −11°. These features lead to a rather inefficient propagation of the superexchange *via* this bridging network, which explains the rather low isotropic interaction constant.

The detailed study of such tris(μ-N^1,N^2-(4*R*)-1,2,4-triazole) copper(II) compounds is extremely worthwhile in view of a better understanding of the Fe(II) analogues, which are well-known to exhibit cooperative spin-crossover behavior.[10−22] Unfortunately, up to now no X-ray crystallographic data could be obtained for these Fe(II) materials. However, the EXAFS study on the related materials $[Fe(Htrz)_2(trz)](BF_4)$ and $[Fe(Htrz)_3]$-

(52) Bonner, J. C.; Fisher, M. E. *Phys. Rev. A* **1964**, *135*, 640.
(53) Estes, W. E.; Gavel, D. P.; Hatfield, W. E.; Hodgson, D. *Inorg. Chem.* **1978**, *17*, 1415.

$(BF_4)_2 \cdot H_2O$ (Htrz = 1,2,4-(4*H*)-triazole; trz = 1,2,4-triazolato) confirms that a similar structure can indeed be formed with Fe(II).[34] Only recently, a detailed EXAFS study finally allowed one to acquire direct information on the effect of Fe(II) spin transition on the spatial and electronic structure of $[Fe(NH_2trz)_3](anion)_2$ (NH_2trz = 4-amino-1,2,4-triazole; anion = NO_3^-, BF_4^-, Br^-, ClO_4^-) and the magnetically diluted phases $[Fe_xZn_{1-x}(NH_2trz)_3](NO_3)_2$.[54−56] In these compounds, the Fe(II) ions are linked by triple N^1,N^2-1,2,4-triazole bridges. This direct linkage of the Fe(II) centers results in a large cooperativity of the spin-crossover behavior, and therefore, considerable hysteresis has been found in these materials.[10−22]

The Cu(II) ion is in a Jahn−Teller-distorted octahedral environment, which is also the origin for two out of three 1,2,4-triazoles linking the metal(II) ions in a very asymmetric fashion with respect to the bond distances. The third ligand binds the metal(II) ions in a more symmetric fashion. In all cases, differences in Cu−N−N angles as well as considerable Cu−N−N−Cu torsion angles are observed. It is important to notice that even though the Cu(II) ions are in Jahn−Teller-distorted octahedra, the chain only shows a relatively small deviation from linearity.

Clearly, the coordination geometry involving the Fe(II) ion should be closer to a regular octahedron, especially for the low-spin state. Indeed, this may be concluded from the structure of the linear trinuclear Fe(II) compound $[Fe_3(4\text{-ethyl-}1,2,4\text{-triazole})_6(H_2O)_6](CF_3SO_3)_2$, where the central Fe(II) ion in the high-spin as well as in the low-spin state is in an almost regular octahedron.[28] Therefore, the bridging N^1,N^2-1,2,4-triazole ligands are all symmetry related, *i.e.*, all ligands are identical and link the Fe(II) ions in a fairly symmetric way with Fe−N−N angles of 124.3(4)° and 124.5(4)° for the high-spin state and 123.6(5)° and 126.1(5)° for the low-spin state. Also, the central high-spin $Fe(II)N_6$ chromophores in $[Fe_3(4\text{-}(p\text{-methoxyphenyl})\text{-}1,2,4\text{-triazole})_6(H_2O)_6](tosylate)_2 \cdot 2CH_3OH \cdot 8H_2O$[32] and $[Fe_3(4\text{-isopropyl-}1,2,4\text{-triazole})_6(H_2O)_6](tosylate)_2 \cdot 2H_2O$[30] have a fairly regular octahedral symmetry. On the contrary, the central high-spin Fe(II) ion in the linear trinuclear compound $[Fe_3(4\text{-}(p\text{-methoxyphenyl})\text{-}1,2,4\text{-triazole})_8(H_2O)_4](BF_4)_2 \cdot 2H_2O$[32] shows a slight Jahn−Teller distortion involving two pairs of Fe−N distances of 2.24(1), 2.14(1), and 2.15(1) Å.

The present EXAFS study is an important step forward in the structural investigation of these linear-chain compounds. For the first time, it has been possible to calculate an ab-initio EXAFS FEFF model for such a compound, which could be compared to its crystal structure. In two previous publications,[34,35] we have indicated that all low-spin Fe(II) linear chains of derivatives of 1,2,4-triazole studied up to now exhibit the so-called 7 Å peak. Definitely, this peak is not an experimental error or data treatment artifact but reflects a structural feature. It is important to notice that this peak has not been observed for the mononuclear compound $[Fe(1\text{-propyl-tetrazole})_6](BF_4)_2$.[35] Therefore, it may be concluded that this 7 Å peak is the signature of the polymeric structure. Other compounds having metal−metal distances of 3−4 Å involving metal alignments, Ni(II)-$(glyoxime)_2$ and Ni(II)$(dimethylglyoxime)_2$, have also been studied by EXAFS: the double metal−metal multiple scattering signal was always observed when the spectra were recorded at low temperature.[35]

The present work may be considered as the final step in this EXAFS study allowing us to compare the EXAFS spectra of the Fe(II) species with a known related structure. The comparison of the thermal behavior of the 7 Å peak in the Fe(II) and Cu(II) compounds is of particular interest. One of the unsolved questions in a previous paper[34] dealt with the disappearance of the signal corresponding to the multiple scattering Cu−Cu−Cu signal in the related Fe(II) high-spin species. The reason for this behavior was not totally clear, since the amplitude of a multiple scattering EXAFS contribution is sensitive to both the scattering angle and the value of the Debye−Waller factor. Even if an alignment of the metal centers is required for a significant multiple scattering contribution, it is possible to smear out an EXAFS peak just by increasing the thermal vibration coefficient without changing the geometry of the metal alignment. This is exactly what is observed for $[Cu(hyetrz)_3](ClO_4)_2 \cdot 3H_2O$, and this effect could be similar in the case of the iron(II) derivatives. Up to now, the EXAFS alignment signature for the Fe(II) polymers has only been detected in the low spin-state, regardless of which temperature the low-spin Fe(II) EXAFS spectrum has been recorded. Indeed, the corresponding multiple scattering signal has been found to be present from 10 to 350 K for various low-spin Fe(II) linear chains.[34] In particular, for $[Fe(Htrz)_2(trz)](BF_4)$,[34] it has been possible to record the EXAFS spectra for the low-spin and high-spin state within the hysteresis loop at the same temperature (355 K). Under these conditions, the multiple scattering Fe−Fe−Fe signal is almost undetectable in the high-spin state but clearly detected in the low-spin state. This is why a structural change from a linear Fe−Fe−Fe chain to a zig-zag structure was proposed as an alternative explanation opposed to a simple increase of the Debye−Waller factor.

In contrast to Cu(II) and high-spin Fe(II), low-spin Fe(II) does not exhibit any Jahn−Teller effect. Evidently, the Jahn−Teller effect is not only responsible for a distortion from octahedral symmetry (static Jahn−Teller) but also leads to an important increase of the vibrational entropy of the compound (dynamic Jahn-Teller). Thus, an important increase of the Debye−Waller factor, without any change of the average Fe−Fe−Fe alignment in Fe(II) high-spin compounds, is consistent with the result obtained in this work for the Cu(II) derivative. It should be pointed out that up to now the EXAFS spectra for the Fe(II) high-spin derivatives have only been recorded for compounds where the LS → HS transition occurs at temperatures higher than 350 K.

The definite EXAFS evidence that the high-spin Fe(II) compounds may possesss a linear structure will only be obtained if an Fe−Fe−Fe multiple scattering EXAFS signature around 7 Å will be found for a high-spin derivative at low temperature (liquid nitrogen or below). This extremely appealing aspect of our structural studies on this type of polymeric Fe(II) compounds is currently in progress.

Acknowledgment. We are very grateful to the staffs of the linear accelerator and storage ring at LURE. We would also like to express our gratitude to Dr. F. Villain for her help in EXAFS data recording and to Dr. D. Watkin for usefull discussions concerning the structure determination.

Supporting Information Available: Tables of detailed structure determination, hydrogen coordinates, anisotropic displacement parameters, bond distances and angles, and hydrogen bonds (9 pages). Ordering information is given on any current masthead page.

IC970895P

(54) Bausk , N. V.; Érenburg, S. B.; Mazalov, L. N.; Lavrenova, L. G.; Ikorskii, V. N. *J. Struct. Chem.* **1994**, *35*, 509.
(55) Bausk, N. V.; Érenburg, S. B.; Lavrenova, L. G.; Mazalov, L. N. *J. Struct. Chem.* **1995**, *36*, 925.
(56) Érenburg, S. B.; Bausk, N. V.; Varnek, V. A.; Lavrenova, L. G. *J. Magn. Magn. Mater.* **1996**, *157/158*, 595.